Journal of Thermal Analysis and Calorimetry (2022) 147:6893–6900
https://doi.org/10.1007/s10973-022-11282-y

Thermal analysis model of scroll compressor with clearance leakage based on multiple scale method

Dou Qin[1] · Bin Zhao[1] · Diankui Gao[1] · Lizhi Xu[1]

Received: 5 May 2021 / Accepted: 17 February 2022 / Published online: 9 March 2022

Abstract
The leakage of scroll compressor can reduce the working efficiency and cause risk, it is significant to study it in depth, thermal analysis of leakage flow of scroll compressor is important to obtain the leakage mechanism. The thermal problem of the scroll compressor in case of clearance leakage is complex, which has strong nonlinear characteristics; therefore, Symlet finite element model with high accuracy and efficiency is established that is applied to analyze thermal performance. The control equation of the scroll compressor is established based on large eddy simulation, and the Symlet finite element model is deduced. The Symlet 10 is selected through error and efficiency comparisons of analyzing a classic heat transfer problem. The accuracy and efficiency of the Symlet 10 finite element model are validated through comparison among three numerical methods. The thermal analysis results based on the proposed Symlet 10 finite element model are closer to real value that other methods, and the computing time of Symlet 10 finite element model is least than other methods. In addition, the effect of axial and radial clearances on temperature of compressor is analyzed. Analysis results can be favorable for optimal design of the scroll compressor.

Keywords Scroll compressor · Clearance leakage · Symlet 10 finite element · Large eddy simulation

Introduction

The scroll compressor is the latest displacement compressor, which has the merits of small occupied space, light weight, high compression efficiency and compact layout. The scroll compressor has established the refrigeration compressor markets depending on variable capacity adjustment technology. Currently the scroll compressor has been going in the direction of broadening the frozen and refrigerated food and heat pump industries. Developing the scroll compressor with better performance and more compact structure is becoming one hot topic of research, where research on heat transfer of the scroll compressor will support optimal design of the scroll compressor. Research on heat transfer mechanism of the scroll compressor has been paid more and more attention by many scientists.

✉ Bin Zhao
zbzbz0203288@163.com

[1] Department of Mechanical Engineering, School of Mechanical Engineering, Liaoning Petrochemical University, Fushun 113001, Liaoning, China

The scroll compressor has a leak between working chamber and outside and between working chambers, and the clearance leakage can influence the performance of the scroll compressor greatly, therefore effect of leakage on heat transfer of the scroll compressor should be studied in depth. The leakage mechanism of the scroll compressor has been widely investigated, and many accomplishments have been obtained.

Fanti Gabriel Rossi et al. studied the effect of flank clearance on performance of scroll expander based on experiment [1]. Singh Simarpreer et al. studied the fluid characteristics of refrigerant in a scroll compressor based on Computational Fluid Dynamics (CFD) method, results showed that the internal leakage of refrigerant could increase the overall efficiency of the scroll compressor [2]. Rak and Pietrowicz studied the effect mechanism of specific parameters on the thermal balance inside of a working chamber with tangential leakages [3]. Fukuta Mitsuhiro et al. studied the leakage characteristics of tip seal in the scroll compressor based on experiment [4]. As seen from the existing researches, the heat transfer analysis of the scroll compressor considering clearance leakage is very less, however the clearance leakage has important effect

on heat transfer process of the scroll compressor. The current research of the scroll compressor are still focus on influence of leakage flow on performance of it, and few studies on influence of leakage flow on heat transfer of it have been conducted. Influence of clearance leakage on the thermal characteristics of the scroll compressor should be studied.

The thermal problem of the scroll compressor in case of clearance leakage has strong nonlinear features, therefore an advanced numerical calculation tool should be used. Wavelet finite element method is a good choice, in recent years, people have conducted more thorough research on the wavelet finite element method, and achieved many fruits.

Azdoud Yan et al. carried out micro-mechanical analysis of poly-crystalline micro structures of metals and alloys based on wavelet finite element model. Various validation tests were carried out to verify the effectiveness of the proposed model [5]. Shen Wei et al. applied B spline wavelet finite element to analyze 2D wave propagation, analysis results showed B spline wavelet finite element method has high accuracy [6]. Zhi-Bo Yang et al. studied the applied wavelet finite element to analyze complex heat conduction problem, and validated the effectiveness of the proposed model [7]. Xiaofeng Xue et al. proposed a Hermitian wavelet finite element model that could deal with wave motion problem successfully [8]. Moreover, the wavelet is biorthogonal, compact supported, and approximate symmetric among the numerous wavelet bases, the Symlet has linear phase, smooth and simple calculation properties [9, 10], therefore the Symlet scale function can be used as interpolation function to construct the Symlet Finite Element Method (SFEM) to improve computational effectiveness.

The existing literatures have concerned the thermal analysis [11–15], however, the effect of leakage flow on thermal characteristics of scroll compressor is not studied in depth, therefore, this research aims to construct thermal model of the scroll compressor considering leakage flow. To improve the computing precision and efficiency, the SFEM has good adaptive ability than traditional finite element method, it is feasible tool for coping with thermal model of the scroll compressor considering leakage flow.

Thermal model of scroll compressor under leakage flow

Control equation

Conservation equation

Continuity equation takes the following form [16]

$$\frac{\partial \rho}{\partial t} + \frac{\partial(\rho u_{\mathrm{i}})}{\partial x_{\mathrm{i}}} = 0, \tag{1}$$

where u_{i} represents the velocity in $i = x$, y and z.

Momentum equation takes the following form [17]

$$\frac{\partial(\rho u_{\mathrm{i}})}{\partial t} + \frac{\partial(\rho u_{\mathrm{i}} u_{\mathrm{j}})}{\partial x_{\mathrm{j}}} = \frac{\partial}{\partial x_{\mathrm{j}}}\left(\mu \frac{\partial u_{\mathrm{i}}}{\partial x_{\mathrm{j}}}\right) - \frac{\partial p}{\partial x_{\mathrm{j}}}, \tag{2}$$

where ρ represents density, μ represents kinetic viscosity, p represents the pressure.

Energy equation takes the following form [18]

$$\frac{\partial T}{\partial t} + \frac{\partial(\rho u_{\mathrm{j}} T)}{\partial x_{\mathrm{j}}} = \frac{\partial}{\partial x_{\mathrm{i}}}\left(\frac{\lambda}{c_p}\frac{\partial T}{\partial x_{\mathrm{j}}}\right), \tag{3}$$

where c_{p} represents specific heat capacity, λ represents heat conductivity, T represents the temperature.

Large eddy simulation (LES)

Clearance leakage flow is affected by boundary layer, main stream and second flow of channel, and is impacted by unsteady aerodynamic characteristic formed periodic exhaust process of the scroll compressor. Therefore, clearance leakage flow can be considered as the turbulent flow, LES is used to describe clearance leakage flow. The filtering processing is carried out for the control equations.

The filter mass equation of LES takes as following form [19]

$$\frac{\partial \overline{\rho}}{\partial t} + \frac{\partial(\overline{\rho u}_{\mathrm{i}})}{\partial x_{\mathrm{i}}} = 0, \tag{4}$$

where $\overline{\rho}$ represents filtered density, $\overline{u}_{\mathrm{i}}$ represents filtered velocity component.

The filtered momentum equation of LES takes as following form [20]

$$\frac{\partial(\overline{\rho u}_{\mathrm{i}})}{\partial t} + \frac{\partial(\overline{\rho u}_{\mathrm{i}}\overline{u}_{\mathrm{j}})}{\partial x_{\mathrm{j}}} = \frac{\partial}{\partial x_{\mathrm{j}}}\left(\mu \frac{\partial \overline{u}_{\mathrm{i}}}{\partial x_{\mathrm{j}}}\right) - \frac{\partial \overline{p}}{\partial x_{\mathrm{j}}} - \frac{\partial \tau_{\mathrm{ij}}}{\partial x_{\mathrm{j}}}, \tag{5}$$

where $\overline{u}_{\mathrm{j}}$ represents filtered velocity component, $j = x$, y and z, $\overline{p}$ represents filtered pressure, τ_{ij} represents sub-grid scale stress, which takes as following form

$$\tau_{\mathrm{ij}} = -2\mu_{\mathrm{s}}\overline{S_{\mathrm{ij}}} + \frac{1}{3}\tau_{\mathrm{kk}}\delta_{\mathrm{ij}}, \tag{6}$$

where μ_{s} represents the sub-grid eddy viscosity coefficient, which is calculated by [21]

$$\mu_{\mathrm{s}} = \rho C_{\mathrm{d}} \Delta^2 |\overline{S}_{\mathrm{ij}}|, \tag{7}$$

where

$$C_{\mathrm{d}} = \frac{< L_{\mathrm{ij}} M_{\mathrm{ij}} >}{< M_{\mathrm{ij}} M_{\mathrm{ij}} >}, \tag{8}$$

where L_{ij} represents the turbulent stress of solvable size Interaction, M_{ij} represents variable relating to filtering scale and shear rate tensor, Δ represents the filtering scale.

$\overline{S_{\mathrm{ij}}}$ represents deformation rate tensor, which is expressed by [22]

$$\overline{S}_{\mathrm{ij}} = \frac{1}{2}\left(\frac{\partial \overline{u}_{\mathrm{i}}}{\partial x_{\mathrm{j}}} + \frac{\partial \overline{u}_{\mathrm{j}}}{\partial x_{\mathrm{i}}}\right), \tag{9}$$

The energy equation of LES takes as following form [23]

$$\frac{\partial \overline{T}}{\partial t} + \frac{\partial(\rho \overline{u}_{\mathrm{j}} \overline{T})}{\partial x_{\mathrm{j}}} = \frac{\partial}{\partial x_{\mathrm{i}}}\left(\frac{\lambda}{c_{\mathrm{p}}} \frac{\partial \overline{T}}{\partial x_{\mathrm{j}}}\right) - \frac{\partial q_{\mathrm{j}}}{\partial x_{\mathrm{j}}}, \tag{10}$$

where $q_{\mathrm{j}} = \overline{u_{\mathrm{j}} T} - \overline{u}_{\mathrm{j}} \overline{T}$.

The linear eddy viscosity model takes as following form

$$\tau_{\mathrm{ij}} - \frac{1}{3}\tau_{\mathrm{kk}}\delta_{\mathrm{ij}} = 2\nu_{\mathrm{t}}\overline{S}_{\mathrm{ij}} = 2C\Delta^2\sqrt{2\overline{S}_{\mathrm{ij}}\overline{S}_{\mathrm{ij}}}\overline{S}_{\mathrm{ij}}, \tag{11}$$

where C represents the model coefficient, $C = 0.09$.

Heat transfer model of scroll compressor

The transient heat model of the scroll compressor takes as following form [24]

$$\rho c_{\mathrm{p}} \frac{\partial T'}{\partial t} - \frac{\partial}{\partial x_{\mathrm{i}}}\left(k_{\mathrm{i}} \frac{\partial T_{\mathrm{i}}'}{\partial x_{\mathrm{i}}}\right) - \rho Q = 0, \tag{12}$$

where k_{i} represents heat conductivity, Q represents the internal heat source of medium in cavity; t represents time, s.

The boundary conditions of heat transfer model are listed as follows:

1. First boundary condition (Γ_1):

$$T'(x, y, z, t) = T_{\mathrm{b}}(t), \tag{13}$$

2. Second boundary condition (Γ_2):

$$k_{\mathrm{x}} \frac{\partial T'}{\partial x} n_{\mathrm{x}} + k_{\mathrm{y}} \frac{\partial T'}{\partial y} n_{\mathrm{y}} + k_{\mathrm{z}} \frac{\partial T'}{\partial z} n_{\mathrm{z}} = \tilde{q}_{\mathrm{f}}(t), \tag{14}$$

3. Third boundary condition (Γ_3):

$$k_{\mathrm{x}} \frac{\partial T'}{\partial x} n_{\mathrm{x}} + k_{\mathrm{y}} \frac{\partial T'}{\partial y} n_{\mathrm{y}} + k_{\mathrm{z}} \frac{\partial T'}{\partial z} n_{\mathrm{z}} = \tilde{h}_{\mathrm{c}}(T_{\mathrm{c}} - T'), \tag{15}$$

where n_{i} ($i = x$, y and z) represents outward cosines; $T_{\mathrm{b}}(t)$ represents the given temperature on Γ_1; $\tilde{q}_{\mathrm{f}}(t)$ represents the given heat flux density on Γ_2; $\tilde{h}_{\mathrm{c}}$ represents the given convective heat transfer coefficient on Γ_3; T_{c} represents ambient temperature.

Heat transfer Symlet wavelet finite element model

Basic characteristics of wavelet

The Symlet wavelet was constructed by Daubechies, which can improve the symmetry of wavelet function while maintaining the simplicity of Daubechies wavelet, so that the Symlet wavelet beet meets the requirements of nonlinear analysis.

The function ψ satisfies the condition $\int_{-\infty}^{+\infty} \psi(x)\mathrm{d}x = 0$, a function can be generated by translation and dilatation that is expressed by [25]

$$\psi_{\mathrm{a,b}}(x) = |a|^{-1/2}\psi\left(\frac{x - b}{a}\right), \quad (a, b \in R, a \neq 0), \tag{16}$$

For arbitrary function $f \in L^2(R)$, if $\psi \in L^2(R)$, the continuous wavelet transform of $f(t)$ is defined by

$$\Psi_{\mathrm{f}}(a, b) = \int_{-\infty}^{+\infty} \overline{\psi_{\mathrm{a,b}}(t)} f(t)\mathrm{d}t, \tag{17}$$

When a and b are discrete values, $a = a_0^{\mathrm{m}}$, $m \in Z$, $b = nb_0a_0^{\mathrm{m}}$, $n \in Z$, the discrete wavelet transform of $f(t)$ are defined by [26]

$$C_{\mathrm{m,n}}(f) = \int_{-\infty}^{+\infty} \overline{\psi_{\mathrm{m,n}}(t)} f(t)\mathrm{d}t, \tag{18}$$

where $\psi_{\mathrm{m,n}}(t) = a^{-\mathrm{m}/2}\psi\left(a_0^{-\mathrm{m}}t - nb_0\right)$, $a_0 > 1, b_0 \neq 0$. The function $\{\psi_{\mathrm{i}}\}_{\mathrm{j}\in\mathrm{J}}$ in Hillbert space is known as a frame. If there are $0 < A, B < \infty$ make following conditions true for all $f \in H$,

$$A\|f\|^2 \leq \sum_{j\in J} |< f, \psi_{\mathrm{j}} >|^2 \leq B\|f\|^2, \tag{19}$$

where A and B are frame limits, if they are equal, the two frames are compact frames. When $\{\psi_{\mathrm{m,n}}\}$, $m, n \in Z$ is a frame of $L^2(R)$, $f(t)$ is expanded to wavelet coefficients by using discrete wavelet transform as coefficient, and the corresponding expression is listed as follows [27]:

$$f(t) = \sum_{m,n} C_{\mathrm{m,n}}(f)\psi_{\mathrm{m,n}}(t), \tag{20}$$

The Symlet wavelet function and its scale function are shown in Figs. 1 and 2.

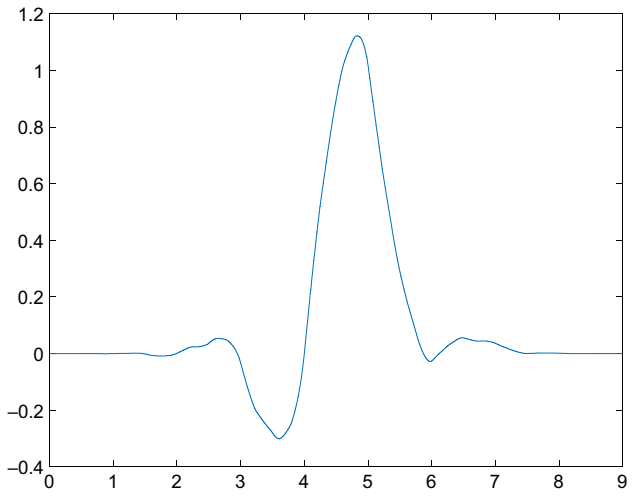

Fig. 1 Symlet wavelet function

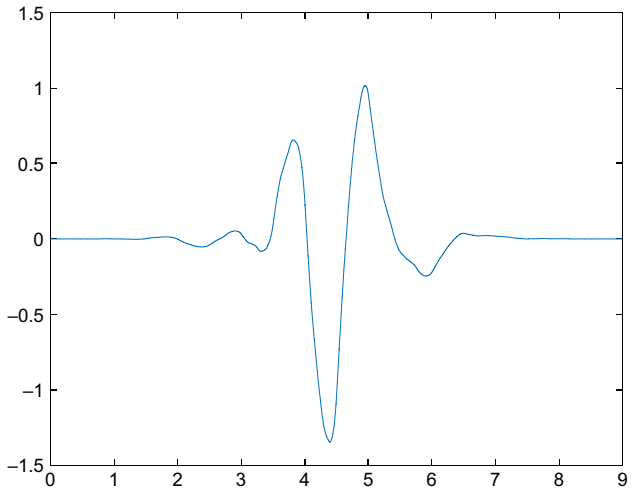

Fig. 2 Symlet wavelet scale function

SFEM

The momentum equation can be changed to following form based on Euler–Taylor–Galerkin method

$$\begin{aligned}
&\int_{V_e}\left(1-\frac{1}{2}\Delta t\mu\frac{\partial^2}{\partial x_i\partial x_i}\right)\frac{u_i^{n+1}-u_i^n}{\Delta t}\Phi_I(b)\mathrm{d}V\\
&=\int_{V_e}\left(1-\frac{1}{2}\Delta t u_j^n\frac{\partial}{\partial x_j}\right)\left(-u_j^n\frac{\partial u_i^n}{\partial x_j}-\frac{\partial p^n}{\partial x_i}+\mu\frac{\partial^2 u_i^n}{\partial x_j\partial x_j}\right)\Phi_I(b)\mathrm{d}V\\
&+\int_{V_e}\frac{1}{2}\Delta t\left[\left(u_k^n\frac{\partial u_j^n}{\Delta x_k}+\frac{\partial p^n}{\partial x_j}-\mu\frac{\partial^2 u_j^n}{\partial x_k\partial x_k}\right)\frac{\partial u_i^n}{\partial x_j}-\left(\frac{\partial p^n}{\partial x_i}-\frac{\partial p^{n-1}}{\partial x_i}\right)\frac{1}{\Delta t}\right]\Phi_I(b)\mathrm{d}V,
\end{aligned}\tag{21}$$

The Symlet wavelet basis velocity field function is expressed by [28]

$$\vec{u}^e=\Phi_J[\vec{u}_J^n]^e,\tag{22}$$

$$\vec{T}^e=\Phi_J[\vec{T}_J^n]^e,\tag{23}$$

where Φ represents Symlet wavelet basis function.

The following expression can be obtained through substituting expression (22) into expression (21):

$$A_{IJ}^e[\vec{u}_J^{n+1}]^e=(B_{IJ}^e[\vec{u}_J^n]^e+C_{IJ}^e[\vec{u}_J^n]^e+P_{IJ}^e+F_I^e)\Delta t+A_{IJ}^e[\vec{u}_J^n]^e,\tag{24}$$

$$A_{IJ}^e=\int_{V_e}\Phi_I T_{fJ}\mathrm{d}V+\int_{V_e}\frac{1}{2}\mu\Delta t\frac{\partial\Phi_I}{\partial x_i}\frac{\partial\Phi_J}{\partial x_i}\mathrm{d}V,\tag{25}$$

$$B_{IJ}^e=\int_{V_e}\left(-\Phi_I u_j\frac{\partial\Phi_I}{\partial x_j}-\mu\frac{\partial\Phi_I}{\partial x_i}\frac{\partial\Phi_J}{\partial x_i}\right)\mathrm{d}V-\int_{V_e}\frac{1}{2}\Delta t u_j u_j\frac{\partial\Phi_I}{\partial x_j}\frac{\partial\Phi_J}{\partial x_j}dV,\tag{26}$$

$$C_{IJ}^e=\int_{V_e}\frac{1}{2}\Delta t\Phi_I\left[\left(u_k\frac{\partial u_j}{\partial x_k}+\frac{\partial p}{\partial x_j}-\mu\frac{\partial^2 u_j}{\partial x_k\partial x_k}\right)\frac{\partial\Phi_J}{\partial x_j}\right]\mathrm{d}V,\tag{27}$$

$$P_{IJ}^e=\int_{V_e}\left[-\frac{1}{2}\left(\frac{\partial p^n}{\partial x_i}-\frac{\partial p^{n-1}}{\partial x_i}\right)\right]\Phi_I\mathrm{d}V,\tag{28}$$

$$F_I^e=\int_{V_e}\left(\Phi_I+\frac{1}{2}\Delta t u_j\frac{\partial\Phi_I}{\partial x_j}\right)\left(-\frac{\partial p}{\partial x_i}\right)\mathrm{d}V,\tag{29}$$

Global finite element equation takes following form

$$A\vec{u}^{n+1}=(B\vec{u}^n+C\vec{u}^n+P+F)\Delta t+A\vec{u}^n.\tag{30}$$

Heat transfer finite element model of scroll compressor

Symlet function is used as interpolation function, and the temperature function takes as following form

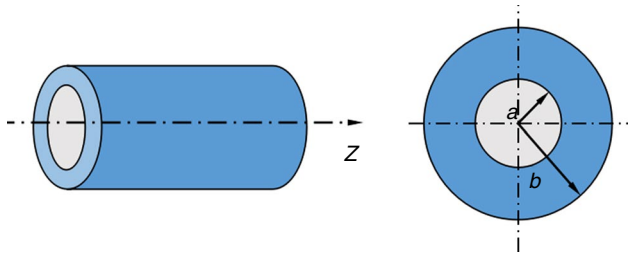

Fig. 3 Diagram of cylinder

$$\vec{T} = \Phi\vec{c}, \tag{31}$$

where $\vec{c} = (c_0, \ldots, c_{-(N-2)})$ is the Symlet coefficient vector.

Equivalent integral form of 3D heat conduction is expressed by [29]

$$\int_{V_e}\left[\delta T'\left(\rho c_T\frac{\partial T'}{\partial t}\right) - \frac{\partial \delta T'}{\partial x}\left(k_x\frac{\partial T'}{\partial x}\right) - \frac{\partial \delta T'}{\partial y}\left(k_y\frac{\partial T'}{\partial y}\right) - \frac{\partial \delta T'}{\partial z}\left(k_z\frac{\partial T'}{\partial z}\right) - \delta T'\rho Q\right]dV - \int_{\Gamma_{2e}}\delta T' q\mathrm{d}S - \int_{\Gamma_{3e}}\delta T h(T_c - T')\mathrm{d}S = 0, \tag{32}$$

where e represents element, V represents element volume, S represents surface of element.

SFEM equation takes as following form

$$H\frac{\mathrm{d}T'}{\mathrm{d}t} + KT' = R, \tag{33}$$

where H is the heat capacity matrix, K is heat conduction matrix, R is the temperature load vector.

Heat transfer analysis of scroll compressor in case of clearance leakage

To validate accuracy of proposed SFEM, a case with exact solution is used to carry comparison analysis. A cylinder that is shown in Fig. 3 is heated from a uniform temperature, temperature of internal surface ($r = a$, $a = 10$ m) of the cylinder increases 10 °C, temperature of outer surface ($r = b$, $b = 20$ m) of the cylinder increases 20 °C, and there is no hot source.

The specifications of the used computer are set as follows: the central processing unit (CPU) is 64 bit, it has 2 core, the memory is 1G, the resolution ratio is 1680, and the memory is 8G.

The temperature along radial direction is calculated by theoretic formulas and SFEM respectively, in order to verify the effectiveness of SFEM, the traditional finite element method is also used to analyze the same problem [30], and comparison results are illustrated in Table 1.

As seen from Table 2, the temperature solution from SFEM is close to exact solution from theoretical model, the calculating errors range from 2.3 to 3.2% when the value of r is different. Therefore the SFEM obtains high computing precision.

Table 1 Comparison results of temperature distribution of cylinder along radial direction

r/mm	Exact solution/°C	Symlet wavelet finite element solution		Traditional finite element solution	
		Simulation value/°C	Error/%	Simulation value/°C	Error/%
12	12.63	13.03	3.2	13.19	4.4
14	14.85	15.22	2.4	15.46	4.1
16	16.78	17.16	2.3	17.52	4.4
18	18.48	18.95	2.5	19.12	3.5

Heat transfer analysis of a scroll compressor in case of leakage is carried out based on SFEM. The inlet pressure is 0.15 MPa, the exhaust pressure is 0.65 MPa, the suction temperature is 293 K, the basic circle radius is 2.8 mm, the number of scroll circles is 3.886, the scroll pitch is 17.26 mm, the rotating radius is 5.86 mm, the thickness of scroll plate is 3.56 mm, the height of the scroll wrap is

Table 2 Mesh of the solution region

Method	Number of elements	Number of nodes
TFEM	96,337	217,732
DFEM	6893	12,886
SW10FEM	4955	8961

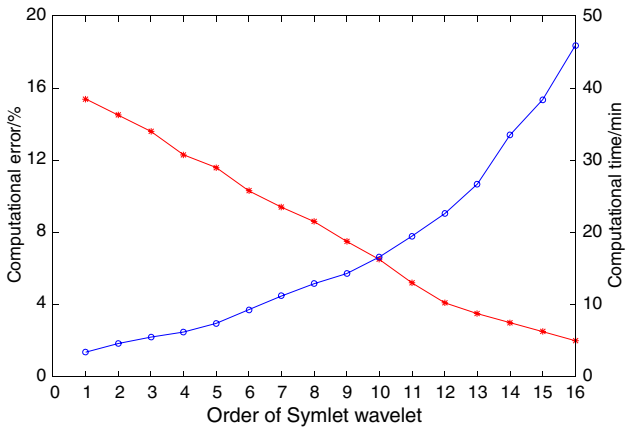

Fig. 4 Computational error and time of different Symlet wavelet function

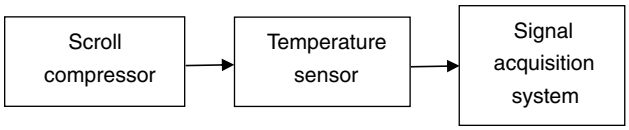

Fig. 5 Temperature testing system of scroll compressor

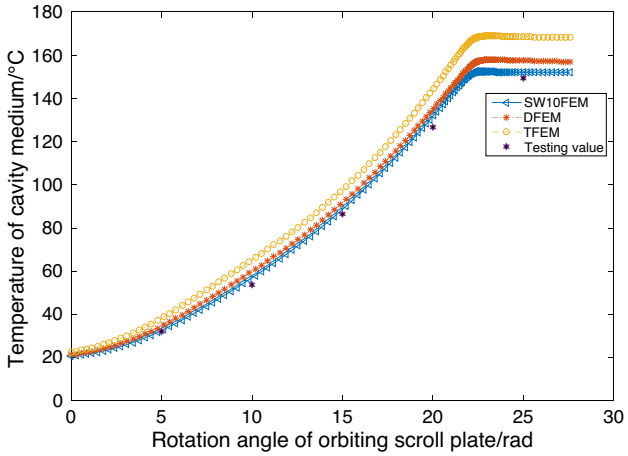

Fig. 6 Temperature changing rules of the scroll compressor by different methods

45 mm, the occurrence angle of involute is 0.65 rad, the termination angle of the scroll teeth is 2.5 rad, and the compression ratio is 4.77. The axial meshing clearance is 0.6 mm, the radial meshing clearance is 0.3 mm.

The Symlets (1–16) are selected to constructed the SFEMs. The computational error and computational time of different Symlets are shown in Fig. 4. As seen from Fig. 4, computational error decreases with order, while the computational time increases with order, the Symlet 10 finite element model can obtain the best analysis effect, which has relatively small calculating errors and calculating time. Therefore, the Symlet 10 finite element (S10FEM) is applied in this research.

To validate effectiveness of the proposed SW10FEM, the traditional finite element method (TFEM), and the Daubechies finite element method (DFEM) are also applied to analyzed the same problem. Mesh generation situations of the solution region are listed in Table 2.

The effect of clearance flow on temperature of cavity of the scroll compressor studied based on TFEM, DFEM and SW10FEM, respectively. To verify the precision of numerical method, the temperature of scroll compressor is also measured by temperature sensor. The testing system is shown in Fig. 5.

The comparison results are illustrated in Fig. 6. From Fig. 6, the temperature of the scroll compressor obtained from SW10FEM comes closer to testing result than that from TFEM and DFEM, the temperature of the cavity medium

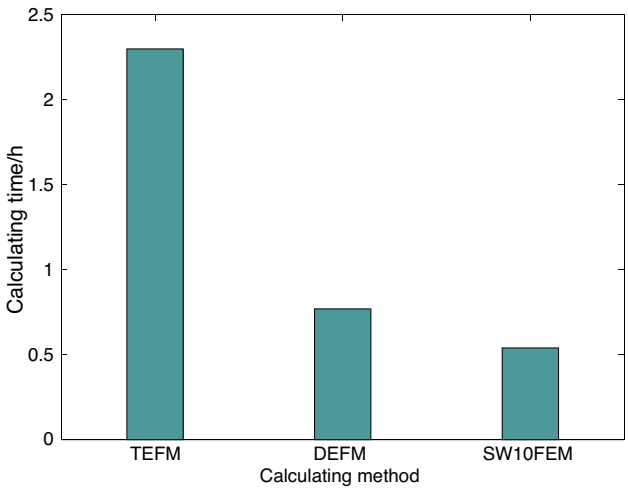

Fig. 7 Running time of different simulation methods

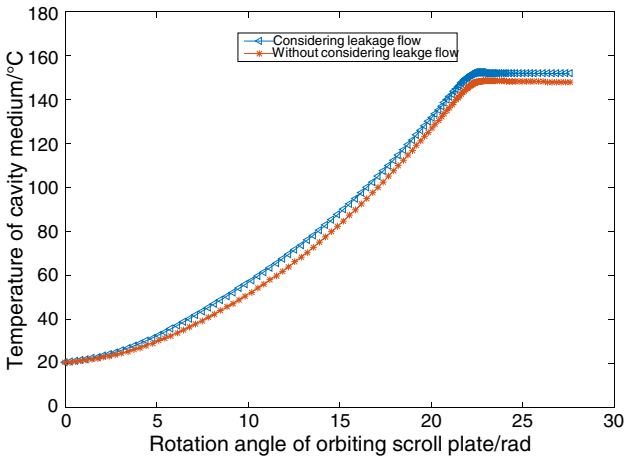

Fig. 8 Temperature changing rules of cavity medium considering and without considering leakage flow

obtained from DFEM is slightly higher than that obtained from SW10FEM, and the solutions obtained from TFEM is lowest, therefore the SW10FEM has higher computational precision than other two methods.

The computing efficiency is also an important evaluation index for heat transfer analysis based on above three numerical methods, the calculating time of different simulation method is illustrated in Fig. 7.

As seen from Fig. 7, running time of TFEM is 2.3 h, which is far greater than that of other two methods, the calculating time of SW10FEM is least, which is 0.54 h; The calculating time of DFEM is between that of other two methods. The analysis results indicate that S10FEM is the best in efficiency, which can save CPU cost.

Heat transfer analysis of the scroll compressor considering leakage flow and without considering leakage flow is,

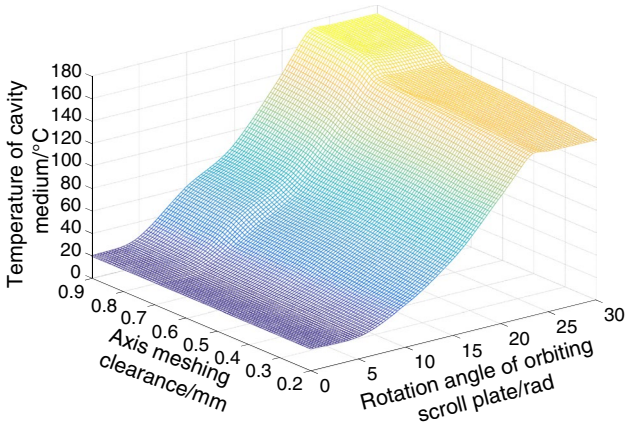

Fig. 9 Effect of axial clearance on temperature

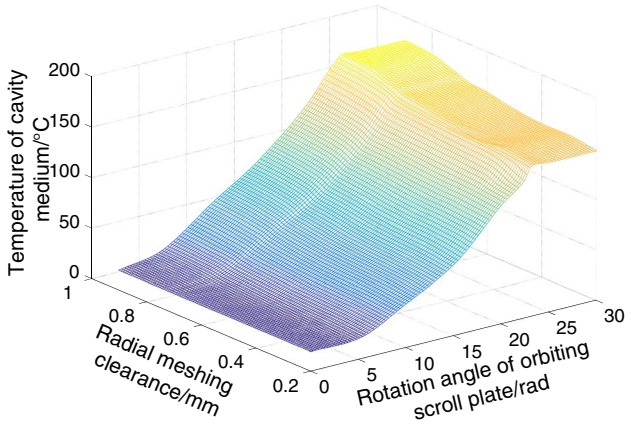

Fig. 10 Effect of radial clearance on temperature

respectively, carried out based on SW10FEM. Simulation results are illustrated in Fig. 8. From Fig. 8, the temperature of scroll compressor considering leakage is higher than that without considering leakage, because the gas at high temperature in high-pressure cavity leaks into the cavity with leakage flow, and then the temperature of the cavity medium with leakage flow is higher than that without leakage flow. The cavity medium can also absorb heat from high-pressure cavity through wall of scroll teeth, therefore, the temperature of compressor increases.

The axial and radial clearances can affect thermal performance of the scroll compressor, effect of axial radial clearances on heat transfer performance is analyzed based on SW10FEM. And the simulation results are illustrated in Figs. 9 and 10. Figure 9 shows effect of axis clearance and rotation angle of orbiting scroll plate on temperature, the temperature of the scroll compressor increases with axis clearance, the main reason for this change is that the heat leaking into the low pressure cavity from high pressure cavity increases with increasing of axis meshing clearance. Figure 10 shows the influences of radius meshing clearance and rotation angle of orbiting scroll plate on temperature of the scroll compressor, the temperature also increases with radius clearance, the temperature rising extent of cavity medium due to radius meshing clearance is higher than that due to axis meshing clearance, because the turbulence intensity in radius meshing clearance is higher than that in axis meshing clearance, therefore the velocity gradient of medium in radius meshing clearance is bigger than that in axial meshing clearance.

The temperature distribution of single working chamber of the scroll compressor is relative uneven, and temperature close to the centre of working chamber is relative high, and the uneven temperature distribution is main decided by clearance leakage of the scroll compressor.

Conclusions

Heat transfer model of the scroll compressor in case of clearance leakage is established, and S10FEM is established that is used to implement heat transfer analysis of the scroll compressor in case of flow. The influence mechanism of clearance leakage flow on temperature of the scroll compressor is revealed.

First, the Symlet wavelet 10 is selected from Symlet wavelet (1–16) to construct S10FEM through comparative analysis of different orders of Symlet wavelets on calculating errors and calculating time. Temperature of scroll compressor obtained from SW10FEM comes closer to testing result than that from TFEM and DFEM, the temperature of the cavity medium obtained from DFEM is slightly higher than that obtained from SW10FEM, and the solutions obtained from TFEM is lowest. The S10FEM can obtain best analysis effect comparing with DFEM and TFEM, which has relatively small calculating errors and calculating time.

Second, heat transfer analysis of the scroll compressor considering and without considering leakage flow is implemented based on proposed model, numerical results illustrate temperature of the scroll compressor considering leakage flow is higher than that without considering leakage flow. The cavity medium can also absorb heat from high-pressure cavity through wall of scroll teeth.

Finally, effect of axial and radial clearances on heat transfer performance of the scroll compressor are analyzed based on SW10FEM. Results show that the temperature of the scroll compressor increases with axis clearance and radius clearances, and temperature rising extent of cavity medium due to radius meshing clearance is higher than that due to axis meshing clearance.

The analysis model with higher computing precision and efficiency will be developed, and the uncertain factors will be considered to obtain the more accurate results.

Author contributions B is in charge of the model construction, wrote and revised the manuscript. HY takes part in the program design. DK takes part in experiment design and test. LZ takes part in simulation analysis. All authors read and approve the final manuscript.

Funding The research is supported by "Scientific Research Funding Project form the Educational Department of Liaoning Province (No. L2019022)."

Data availability All data are fully available without restriction.

Declarations

Conflict of interest The authors declare no competing financial interest.

References

1. Fanti GR, Romão DA, de Almeida RB, de Mello PEB. Influence of flank clearance on the performance of a scroll expander prototype. Energy. 2020;193:116823.
2. Singh S, Singh A, Dasgupta MS. CFD modeling of a scroll work recovery expander for trans-critical CO_2 refrigeration system. Energy Procedia. 2017;109:146–52.
3. Rak J, Pietrowicz S. Internal flow field and heat transfer investigation inside the working chamber of a scroll compressor. Energy. 2020;202:117700.
4. Mitsuhiro F, Takeru S, Masaaki M. Leakage and friction characteristics at sliding surface of tip seal in scroll compressors. Int J Refrig. 2021;125:104–12.
5. Yan A, Jiahao C, Somnath G. Wavelet-enriched adaptive crystal plasticity finite element model for polycrystalline microstructure. Comput Methods Appl Mech Eng. 2017;327:36–57.
6. Shen W, Li D, Ou J. Dispersion analysis of multiscale wavelet finite element for 2D elastic wave propagation. J Eng Mech. 2020;146(4):04020022.
7. Yang Z-B, Wang Z-K, Tian S-H, Chen X-F. Analysis and modelling of non-Fourier heat behavior using the wavelet finite element method. Materials. 2019;12(8):1337.
8. Xue X, Wang X, Wang Z, Xue W. Wave motion analysis in plane via Hermitian cubic spline wavelet finite element method. Shock Vib. 2020;2020:8752656.
9. Al-Shayea TK, Mavromoustakis CX, Batalla JM, Mastorakis G. A hybridized methodology of different wavelet transformations targeting medical images in IoT infrastructure. Measurement. 2019;148:106813.
10. Ebrahimi M, Sohrabi MR, Motiee F, Davallo M. Rapid simultaneous spectrophotometric determination of acetaminophen, phenylephrine, and guaifenesin in a cold syrup formulation based on continuous wavelet transform and first derivative transform methods. Optik. 2021;230:166323.
11. Acharya N. Spectral simulation to investigate the effects of active passive controls of nanoparticles on the radiative nanofluidic transport over a spinning disk. J Thermal Sci Eng Appl. 2021;13(3):031023.
12 Acharya N, Mondal H, Kundu PK. Spectral approach to study the entropy generation of radiative mixed convective couple stress fluid flow over a permeable stretching cylinder. Proc Inst Mech Eng Part C J Mech Eng Sci. 2020;225:2692–704.
13. Acharya N. Spectral quasi linearization simulation of radiative nanofluidic transport over a bended surface considering the effects of multiple convective conditions. Eur J Mech B Fluids. 2020;84:139–54.
14. Acharya N. Framing the impacts of highly oscillating magnetic field on the ferrofluid flow over a spinning disk considering nanoparticle diameter and solid–liquid interfacial layer. J Heat Transf. 2020;142(10):102503.
15. Acharya N. Spectral simulation to investigate the effects of nanoparticle diameter and nanolayer on the ferrofluid flow over a slippery rotating disk in the presence of low oscillating magnetic field. Heat Transf. 2021;50:5951–81.
16. Hoseinzadeh S, Stephan Heyns P. Thermo-structural fatigue and lifetime analysis of a heat exchanger as a feedwater heater in power plant. Eng Fail Anal. 2020;113:104548.
17. Jordaan H, Stephan Heyns P, Hoseinzadeh S. Numerical development of a coupled one-dimensional/three-dimensional computational fluid dynamics method for thermal analysis with flow maldistribution. J Thermal Sci Eng Appl. 2021;13(4):041017.
18. Wang H, Wang S, Lu D. Large eddy simulation on the heat transfer of supercritical pressure water in a circular pipe. Nucl Eng Design. 2021;377:111146.
19. Wei X, Zhang M, An Z, Wang J, Huang Z, Tan H. Large eddy simulation on flame topologies and the blow-off characteristics of ammonia/air flame in a model gas turbine combustor. Fuel. 2021;298:120846.
20 Hoseinzadeh S, Sohani A, Ashrafi TG. An artificial intelligence-based prediction way to describe flowing a Newtonian liquid/gas on a permeable flat surface. J Thermal Anal Calorim. 2021;147:4403–9.
21. Creech ACW, Jackson A. Hybrid large eddy simulation for low-order discontinuous Galerkin methods using an explicit filter. Comput Phys Commun. 2021;260:107730.
22. Hoseinzadeh S, Sohani A, Shahverdian MH, Shirkhani A, Heyns S. Acquiring an analytical solution and performing a comparative sensitivity analysis for flowing Maxwell upper-convected fluid on a horizontal surface. Thermal Sci Eng Progress. 2021;23:100901.
23 Stieren A, Gadde SN, Stevens RJAM. Modeling dynamic wind direction changes in large eddy simulations of wind farms. Renew Energy. 2021;170:1342–52.
24. Huang T, Diao S, Yang Z, Huang Z, Zhang Y, Zhou H. Flow dynamics and heat transfer characteristics analysis for floatation nozzle using large eddy simulation and proper orthogonal decomposition method. Int J Thermal Sci. 2020;155:106402.
25. Lalithakumari S, Pandian R. Pre processing of ultrasonic signals austenitic stainless steel weld at high temperature. Mater Today Proc. 2020;21:430–3.
26 Awal MA, Mostafa SS, Ahmad M, Rashid MA. An adaptive level dependent wavelet thresholding for ECG denoising. Biocybern Biomed Eng. 2014;34(4):238–49.
27. Borova M, Prauzek M, Konecny J, Gaiova K. Environmental WSN edge computing concept by wavelet transform data compression in a sensor node. IFAC-PapersOnLine. 2019;52(27):246–51.
28. Lu H, Vaz MA, Caire M. Alternative analytical and finite element models for unbonded flexible pipes under axisymmetric loads. Ocean Eng. 2021;225:108766.
29. Qiu H. Multi-level mixed finite element algorithms for the stationary incompressible magneto-hydrodynamics equations. Comput Math Appl. 2021;86:33–48.
30. Hobiny AD, Abbas I. The impacts of variable thermal conductivity in a semiconducting medium using finite element method. Case Stud Thermal Eng. 2022;31:101773.